Received Date : 04-Jul-2016
Revised Date : 19-Sep-2016
Accepted Date : 21-Sep-2016
Article type : Original Article: Experimental Allergy and Immunology

An early innate response underlies severe influenza-induced exacerbations of asthma in a novel steroid-insensitive and anti-IL-5 responsive mouse model.

A novel model of severe exacerbation of chronic asthma.

Lara Ravanetti[1,2], Annemiek Dijkhuis[1,2], Yanaika S. Sabogal Pineros[1,2], Suzanne M. Bal[3], Barbara S. Dierdorp[1], Tamara Dekker[1], Adrian Logiantara[1], **Ian M. Adcock[4]**, Navin L. Rao[5], Louis Boon[6], Gino Villetti[7], Peter J. Sterk[2], Fabrizio Facchinetti[7] and René Lutter[1,2] for the U-BIOPRED Study Group.

1. Department of Experimental Immunology, Academic Medical Centre, Amsterdam 1105AZ, The Netherlands.
2. Department of Respiratory Medicine, Academic Medical Centre, Amsterdam 1105AZ, The Netherlands.
3. Department of Cell Biology and Histology, Academic Medical Centre, Amsterdam 1105AZ, The Netherlands.
4. Airway Disease Section, National Heart & Lung Institute, Imperial College London, Royal Brompton Campus, London SW3 6NP, UK.
5. Immunology Discovery, Janssen Research and Development LLC, San Diego, 92121 CA, USA.
6. Bioceros, Utrecht 3584CM, The Netherlands.
7. Pulmonary Pharmacology Unit, Corporate Pre-Clinical R&D, Chiesi Farmaceutici S.p.A. Parma 43122, Italy.

#Corresponding author mail id: l.ravanetti@amc.nl

Abstract

Background: Acute worsening of asthma symptoms (exacerbation) is predominantly triggered by respiratory viruses, with influenza causing the most severe exacerbations. The lack of an adequate animal model hampers mechanistic insight and the development of new

This article has been accepted for publication and undergone full peer review but has not been through the copyediting, typesetting, pagination and proofreading process, which may lead to differences between this version and the Version of Record. Please cite this article as doi: 10.1111/all.13057
This article is protected by copyright. All rights reserved.

Accepted Article

therapeutics. Aim: We developed and characterized a robust, consistent and reproducible mouse model of severe exacerbation of chronic allergic asthma.

Methods: Chronic allergic airway inflammation was induced following a house dust mite (HDM)-sensitization protocol. HDM-sensitized mice and controls were infected with influenza virus A/X31 H3N2 and either or not treated with inhaled Fluticasone Propionate (FP), systemic corticosteroids (Pred) or anti-IL5. Mice were sacrificed at different time points after infection: cellular accumulation and cytokines levels in the airways; PenH as a measure of airway hyperresponsiveness (AHR); lung histology and viral replication were assessed.

Results: Infection with low dose A/X31 H3N2 led to prolonged deterioration of lung function, aggravated mucus production, peri-vascular, peri-bronchial and allergic inflammation that was unresponsive to inhaled corticosteroids, but responsive to systemic corticosteroids. The exacerbation was preceded at 14h after virus exposure by a marked innate, but no Th2 and Th1 response, subsequently followed by enhanced numbers of eosinophils, neutrophils, dendritic and T cells into the lung lumen, parenchyma and draining lymph nodes in HDM-sensitized mice. Anti-IL-5 treatment attenuated eosinophils and prevented the X31-induced exacerbation.

Conclusions: Together these findings indicate that an early innate response that involves eosinophils underlies the exacerbation. This model recapitulates all major features of severe asthma exacerbations and can serve to discern driving mechanisms and promote development of novel therapeutics.

Introduction

Severe asthma exacerbations are increasingly recognized as one of the major unmet needs in contemporary respiratory medicine[1,2]. The public health burden associated with severe asthma exacerbations has increased worldwide over the past two decades with wide variations in case-fatality across Europe and US[3]. Centers for Disease Control and Prevention in the US estimated that yearly 20% of asthmatics had severe exacerbations requiring high doses of systemic steroids and hospitalization[4].

This article is protected by copyright. All rights reserved.

Accepted Article

Respiratory viruses are the main triggers for asthma exacerbations[5]. Influenza virus exacerbates asthma less frequently than rhinovirus (RV) and respiratory syncytial virus (RSV), but causes the most severe asthma exacerbations[5-7]. This is suggestive of virus-specific immune and inflammatory pathways that determine intensity and duration of an exacerbation[1,8,9]. Current understanding of these pathways in severe asthma exacerbations is fragmentary, which relates to the difficulty in obtaining sequential samples during a severe exacerbation. Key features are early, enhanced neutrophil and eosinophil numbers in the airway lumen and bronchial mucosa, and increased levels of inflammatory mediators such as IL-1β, IL-6, TNF-α and various chemokines[10].

Mild to moderate exacerbations can be treated by quadrupling the maintenance doses of inhaled corticosteroids (ICS), but this is impractical for severe exacerbations as these patients are already treated with high doses of ICS or systemic corticosteroids (SCS). Currently, the only effective treatment for severe exacerbations is provided by high doses of SCS, but with a relatively low efficacy[2,11], and a high risk-benefit ratio[12,13]. As SCS have multiple local and systemic side effects, particularly when used periodically at high doses and over prolonged periods of time, alternative interventions are still desired. Recently, it was demonstrated that Mepolizumab (humanized monoclonal anti-IL-5 antibody) reduced exacerbations in a phenotypically homogeneous cohort of patients with refractory eosinophilic asthma and a history of recurrent severe exacerbations[12,14]. Despite this successful example of biomarker-driven drug development, identification of initial events triggered by viruses that underlie worsening of asthma symptoms may provide alternative therapeutic options and lead to identification of biomarkers predictive of treatment response.

At present, the lack of a consistent and translational animal model of virus-induced severe asthma exacerbations has hampered dissection of the mechanisms underlying exacerbations, the development of new interventions as well as the evaluation of long-term effects of recently developed medication, such as for Mepolizumab. Here we describe a robust mouse model of influenza-induced severe exacerbation of allergic asthma showing a prolonged enhanced airway hyperresponsiveness (AHR), increased mucus production, lung inflammation and pathology with severe structural changes. As noted in severe asthma exacerbations this model displayed a pronounced insensitivity to ICS, whereas the exacerbation phenotype is prevented with SCS or anti-IL5 treatment (TRFK5, anti-mouse/human IL5 antibody). Interestingly, the anti-IL5-mediated eosinophil depletion

This article is protected by copyright. All rights reserved.

Accepted Article

largely affected recruitment of neutrophils, dendritic cells (DC) and CD4+ and CD8+ lymphocytes and enhanced amphiregulin production, despite enhanced viral loads. Corticosteroids exercised similar effects, but decreased the initial viral load. We show that a marked early innate response plays a role in driving the disease and the subsequent enhanced numbers of eosinophils, neutrophils, dendritic and T cells into the airway in HDM-sensitized mice.

This model can be exploited to provide further mechanistic insights, explore novel therapeutic strategies and evaluate long-term treatment effects of intervention.

Results

Influenza aggravates inflammation and airway hyperresponsiveness in house dust mite (HDM)-sensitized mice

Chronic allergic airway inflammation was induced by exposing C57BL/6J mice for five days a week, for five consecutive weeks, to the aeroallergen house dust mite (HDM) via intranasal (i.n.) administration[15,16]. As anticipated, this led to a prominent and persistent eosinophilic allergic inflammation with structural and functional abnormalities of the airways. On the first day of the fifth week of exposure, HDM- or PBS-treated mice were inoculated i.n. with 20 50% tissue-culture infective dose units ($TCID_{50}$) of influenza virus A/X31 H3N2 (X31) or PBS as a control (Supplementary Fig. 1A). After influenza infection, HDM animals (HDM/X31) showed significantly higher (maximally 18%) and prolonged (up to 15 days post-infection) body weight loss, a surrogate marker of inflammation, compared to non-sensitized infected (PBS/X31) and HDM-sensitized non-infected (HDM/PBS) mice (Fig. 1A). HDM/X31 mice also displayed enhanced AHR between day 4-15 post-infection (Fig. 1B, left to right), particularly evident at higher doses of methacholine (Mch).

Differences in the kinetics of immune and inflammatory cell subsets between HDM/X31 and controls may reflect mechanistic differences. Total cell numbers in HDM/X31 mice compared to controls increased biphasically with an early, short (14h), and later, prolonged (4-8 days) cellular accumulation in bronchoalveolar lavage fluid (BALF) and mediastinal draining lymph nodes (mLNs), as opposed to an early, short cellular increase in lung parenchyma (Lung) only (Fig. 2A-C). In BALF the early cell increase was associated with an increased numbers of neutrophils and T lymphocytes (Fig. 2D). The later prolonged phase in BALF started with eosinophils, followed by neutrophils and CD4+ lymphocytes and again

This article is protected by copyright. All rights reserved.

Accepted Article

later DC and CD8+ lymphocytes. The early total cell increase in lung tissue was associated with increased numbers of eosinophils, neutrophils, DC and lymphocytes (Fig. 2E). Similar to this seen in lung parenchyma, also the early cell increase in mLNs was associated with eosinophils, neutrophils, DC and lymphocytes (Fig. 2F). The second phase of cell increase in mLNs was closely similar to the later prolonged phase in BALF.

Interestingly, despite the major changes in the cellular kinetics in HDM/X31 mice, alveolar macrophage (AMΦ) and B cell recruitment were not different from controls (Supplementary Fig. 2A).

Subsequently we evaluated whether cellular responses were paralleled by coherent changes in inflammatory mediator and effector molecule profiles in lung parenchyma and BALF. In BALF from HDM/X31 mice, compared to that of controls, we observed a significant increase at the protein level for the alarmin IL-33 (day 1), the innate cytokines IP10/CXCL10 (day 1 and 2), KC and TNF-α (day 1, 2 and 6), IL-12p40 (day 2, 4 and 8) and the neutrophil effector molecule myeloperoxidase (MPO; day 1, 2, 6 and 8) (Fig. 3A). Notably, IL-33 in lung homogenates from HDM/X31 was markedly increased from day 1 onwards and for all subsequent days tested. At later time points, mediators representative of Th2 and Th1 profiles were significantly induced in lung homogenates from HDM/X31 mice. These included IL-13 (between day 2 to 6), IL-5 (day 6) and anti-viral IFN-γ (day 4 and 6). The chemokines MCP-1/CCL2, MIP-3α/CCL20, RANTES and inflammatory cytokines KC, IL-6, IL-17A, TNF-α were all significantly induced at day 6 after influenza infection in HDM-sensitized mice (Fig. 3B).

Collectively, we show that an exacerbation is preceded by a discriminatory early influx of innate immune cells in HDM/X31 mice. The profound and prolonged body weight loss and deterioration of AHR, reflecting the exacerbation, were paralleled by IL-33 and inflammation in general.

Influenza infection and HDM sensitization synergize in histopathological changes and viral loads

Influenza infection of HDM-sensitized mice as compared to controls led within a day to a more outspoken peribronchial (black arrow) and perivascular (blue arrow) inflammation (Fig. 4A). Similarly, influenza infection enhanced mucus production (magenta) by epithelial goblet

This article is protected by copyright. All rights reserved.

Accepted Article

cells (black arrow) and vascular occlusive lesions (white arrow) in HDM-sensitized mice (Fig. 4B). These early changes did not correlate with the viral load, although there was a delayed viral clearance in HDM/X31 mice at days 4 and 8 post-infection (Fig. 4C). By day 15, influenza X31 had been almost completely cleared, whereas the histopathological changes were still manifest.

Influenza-induced exacerbations in HDM-sensitized mice are not prevented by inhaled Fluticasone Propionate (FP), but are by systemic Prednisone (Pred)

Whereas the inhaled corticosteroid (ICS) FP controls inflammation during stable disease, it does not prevent virus-induced neutrophil and eosinophil recruitment and inflammatory mediator responses in moderate and severe asthma[17]. In our model, FP (300 µg/kg of body mass) was administered i.n. daily during the last 2 weeks of the HDM-sensitization schedule (Supplementary Fig. 1B). FP did not prevent increasing AHR in HDM/X31 mice (Fig. 5A). Neither did FP prevent recruitment of BALF eosinophils, neutrophils, DC and CD4+ T cells in HDM/X31 mice, whereas FP efficiently prevented the recruitment of these BALF cells from PBS/X31 mice (Fig. 5B). Interestingly, CD8+ T cells in BALF from HDM/X31 mice were efficiently attenuated at day 8 after infection by FP (Supplementary Fig. 3). Similar results were obtained for mLNs, although FP reduced recruitment of DC, T (CD8+)- and B-lymphocytes at day 4, but not at later time points (Fig. 5C).

High doses of systemic corticosteroids (SCS) significantly suppress inflammation during severe asthma exacerbations. Prednisone (Pred), given from day 25 of the sensitization schedule onwards (Supplementary Fig. 1C), significantly prevented increasing AHR (Fig. 6A) and recruitment of all cell types in BALF (Fig. 6B) and mLNs (Fig. 6C) in HDM/X31 mice.

Very similar findings were obtained for cells in lung parenchyma (Supplementary Fig. 4).

These findings are in line with failure to prevent virus-induced severe asthma exacerbations by ICS and control by SCS and thereby further validate our model.

Anti-IL-5 attenuates AHR and eosinophils but also modulates other immune and inflammatory cells

Recent trials with anti-IL-5 therapy have highlighted the potential role of anti-IL5 therapy in controlling severe asthma exacerbations, although its mode of action beyond that of attenuation of eosinophils is unclear[18,19]. The murine equivalent (TRFK5) of Mepolizumab as

This article is protected by copyright. All rights reserved.

Accepted Article

opposed to an IgG1 isotype control given on day 26 and 32 of the sensitization schedule (Supplementary Fig. 1D), significantly prevented increasing AHR in HDM/X31 mice (Fig. 7A). As expected, the early eosinophil recruitment in BALF (maximal at day 4 post-infection) was suppressed. Interestingly, TRFK5 treatment significantly enhanced neutrophil numbers at day 4 in BALF from HDM/X31 mice, whereas other cells types remained unaffected (Supplementary Fig. 5). TRFK5 also significantly reduced eosinophils in lung tissue at day 4, but not at day 6. In contrast, TRFK5 significantly reduced neutrophil, DC, total lymphocyte (not shown), CD4+ T cell, CD8+ T cell and B cell (not shown) numbers in lung parenchyma at day 6 post-infection (Fig. 7B). This indicates that TRFK5 treatment is associated with distinct effects on eosinophils and other cell types in the airway lumen and lung parenchyma.

Effect of TRFK5 on viral load

Little is known about the effects of anti-IL5 treatment on viral loads. The viral load in HDM/X31 mice treated with TRFK5 was higher than that in HDM/X31 mice receiving isotype control (Fig. 8A). These data contrast with viral loads in mice treated with FP or with Pred (Fig. 8B and C), which demonstrated a pronounced and modest reduction by Pred and FP in HDM/X31 mice, respectively. Interestingly, FP also reduced the viral load in PBS/X31 mice (Fig. 8B), but HDM sensitization apparently enhanced unresponsiveness to FP whereas Pred could overcome this unresponsiveness.

Amphiregulin production is restored by SCS and TRFK5 treatment

Amphiregulin is an epidermal growth factor (EGF)-like molecule that regulates tissue remodeling and repair in asthma, acute lung epithelial injury and infection[20-22]. Various recent studies have demonstrated that in addition to epithelial and mesenchymal cells, mast cells, basophils, group 2 innate lymphoid cells (ILC2s), and a subset of tissue-resident CD4+ T cells can all express amphiregulin. In view of this we assessed amphiregulin in lung homogenates and BALF samples and observed reduced BALF concentrations between day 2 and 6 in HDM/X31 mice. Interestingly, amphiregulin levels in lung parenchyma did not differ between groups (Fig. 9A). Notably, BALF amphiregulin at day 4 and 6 was significantly increased by treatment with Pred (Fig. 9B), and with TRFK5 (Fig. 9C) in both BALF and lung tissue (day 6) of HDM/X31 mice. This demonstrated that amphiregulin is reduced in HDM/X31 mice, particularly in the airway lumen, but was enhanced again by Pred and TRFK5 treatment.

This article is protected by copyright. All rights reserved.

Accepted Article

Accepted Article

Discussion

A detailed understanding of the pathology of virus-induced severe asthma exacerbations is required for the development of safe and effective interventions and for early recognition of an exacerbation. A validated animal model would greatly contribute to this understanding by enabling in depth kinetic analyses and studies into consequences of interventions. The mouse model presented here comprises all key features of severe exacerbations in allergic asthmatics[2,5,11,23-25] like a prolonged AHR, enhanced neutrophilic and eosinophilic inflammation, enhanced inflammatory mediators known to be associated with exacerbations (IL-33, IL-5 and IL-13)[24], enhanced mucus production by goblet cells, occlusive vascular lesions and un-responsiveness to inhalant corticosteroids and responsiveness to systemic corticosteroids. Anti-IL-5, which has been shown to reduce exacerbations in patients with severe eosinophilic asthma, reduced virus-induced AHR and inflammation in this model in support of its relevance for studying severe exacerbating asthma.

With the detailed follow-up over time we expected to identify processes by which HDM-sensitized mice respond to the viral challenge and that are discriminatory from those by controls. Already fourteen hours after influenza exposure, a set of innate mediators was markedly released in the airway lumen (IL-33, KC, TNF-α, IP10 and IL-12p40) and in lung tissue (IL-33 and IP10). This initial and discriminatory response thus is not an exaggerated Th1 or Th2 adaptive response, but rather an exaggerated innate response. The presence of these mediators in BALF indicates that airway epithelial cells and possibly macrophages mediate this response. After this initial peak of mediators there is a second peak around days 6 and 8, which is predominantly manifest in lung tissue and displays an innate (IL-33, IP-10, TNF-α, MCP-1, IL-6, KC, RANTES), Th1 (IFN-γ) and Th2 (IL-5, IL-13) profile. Further studies are necessary to dissect the source of these mediators, particularly those that are present in the initial peak, and the mechanism that underlies this enhanced release.

The kinetics of myeloid and lymphoid cell subsets was in line with that of chemokines and inflammatory mediators (Fig. 2D-F). Specifically, we found that the kinetics of KC, IL-17 and MPO in BALF paralleled that of the recruitment and activation of neutrophils, changes in RANTES and IL-17 were associated with the recruitment and activation of T lymphocytes and IL-12 correlated most likely with the late induction of Th1-competent CD8+ lymphocytes (Fig. 2D, Fig. 3A). Similarly, in lung parenchyma changes in MCP-1 and MIP-3α preceded the recruitment of DC, whilst a rise in IP10, TNF-α and IFN-γ levels preceded

This article is protected by copyright. All rights reserved.

the recruitment and activation of CD4+ T cells and finally changes in eosinophil numbers paralleled alterations in levels of IL-5 and IL-13 (Fig. 2E, Fig. 3B). Therefore we assume that the enhanced cell numbers are due to recruitment and not to a reduced migration of cells from the lungs.

In line with the aforementioned data, removal of IL-5 depleted eosinophil numbers, particularly those from the initial peak (day 4) both in BALF and lung parenchyma, but not at day 6 (Fig. 7). Intriguingly anti-IL-5 led to enhanced neutrophil numbers in BALF at day 6 (Supplementary Fig. 5) and reduced numbers of neutrophils, DCs, CD4+ and CD8+ lymphocytes at day 6 in lung parenchyma. These findings indicate that IL-5-responsive eosinophils may drive the recruitment of these cells and thus the clinical effects seen during anti-IL-5 treatment may not be due entirely to eosinophils. This may also apply to the anti-IL-5-induced reduction of AHR. That eosinophils can orchestrate immune responses was shown recently[26], as eosinophils controlled the recruitment of CD8+ cells and polarization of macrophages that were critical for cancer eradication. The lack of an effect of anti-IL-5 on lung tissue and BALF eosinophils is suggestive of an anti-IL-5-unresponsive population of eosinophils. These findings warrant a further in depth study into the effects of anti-IL-5.

Interestingly, an increased level of viral replication in HDM-sensitized mice was found, compared to that in PBS-treated animals (Fig. 4C). These findings are in line with increased rhinovirus16 loads in asthma patients subjected to an experimental challenge[24]. In our study we failed to detect the innate interferons (IFN-α and IFN-β), but we did find an enhanced IFN-γ response, also in line with a recent study[27]. Together this indicates that despite the pronounced Th2 inflammation, a proper anti-viral Th1 response is apparent in HDM-sensitized mice. Further analyses revealed that influenza load does not correlate with inflammation and AHR as was quite clear in the anti-IL-5-treated mice (Fig. 8A). In fact, the viral load even increased, which may be explained by the proposed antiviral activity of eosinophils[28-30]. Unexpectedly, we found that Pred treatment attenuated viral load while FP failed to do so in the HDM/X31 mice (Fig. 8B). This finding suggests that corticosteroids may attenuate viral loads particularly during early infection, by an as yet unknown mechanism, and that HDM sensitization interferes with this anti-viral effect of FP (Fig. 8C).

This article is protected by copyright. All rights reserved.

Accepted Article

The EGF-like molecule amphiregulin drives wound repair as well as tissue remodeling by inducing mitosis and by differentiation of epithelial cells and fibroblasts, as reported in acute epithelial injury, asthma, and virus-induced pneumonia[20,21,31]. In HDM/X31 mice amphiregulin levels were significantly reduced, but were restored by systemic prednisone or anti-IL-5 treatment (Fig. 9). This indicates that HDM sensitization suppresses this repair process, but it is not clear which of the amphiregulin-producing cells, i.e. epithelial, mesenchymal and hematopoietic cells are affected. The reduced levels of amphiregulin in the airway lumen in HDM-sensitized mice, with enhanced hematopoietic cell numbers, indicate that amphiregulin is produced predominantly by epithelial cells, but this awaits further study.

Various murine models of virus-induced asthma exacerbations have recently been described that differ from ours in type of allergen and duration of sensitization and in the use of mice strains and of viral challenge. Most presented animal models are based on ovalbumin (OVA) sensitization) [30-32]. In contrast to HDM, which was used here, long-term challenges with OVA might lead to tolerance, downregulation of inflammation and AHR[33-35], even independent of the used mouse strain[15] (and also Dr. Robert Shaw, GSK, unpublished data). Therefore, there is a risk that long-term and/or exaggerated exposure to OVA will adversely affect the response to a viral challenge. This may possibly explain why, in mice exposed to OVA with high concentrations of aluminium hydroxide to boost the Th2 immune response, RSV infection did not induce differential inflammatory cytokines levels, eosinophilic, neutrophilic and lymphocytic influx in airways of OVA-sensitized mice[36]. And similarly, infection with mouse-adapted H1N1 strains led to a reduced airway infiltrate and cytokine production in mice exposed to OVA as compared to controls[37]. Interestingly, challenges with other strains like influenza A pdm09 virus and RV infection of human ICAM-1-expressing mice led to eosinophilia and Th2 cytokine production[32,37]. In contrast to the present study, only few features characteristic of asthma exacerbations were studied in these models. Recently Nguyen and colleagues reported more extensive analyses in RSV challenged OVA-sensitized mice, which shows many parallels with what we report here such as the ICS insensitivity, cell recruitment and cytokine production. In the present study using HDM as an allergen, however, we provide more detail on pathology and the course of the various responses in time. That may be the reason why next to a neutrophilic response we also report an eosinophilic response, but at an earlier time point than studied by Nguyen et al. The same is true for the increases in TNF-α and KC, but our data clearly point to a very early differentiating response for IL-33.

This article is protected by copyright. All rights reserved.

Accepted Article

Other models made use of polyinosinic:polycytidylic acid (poli-I:C), as a surrogate of a viral infection, or Freund's complete adjuvant in combination with HDM leading to a partial boosted airway inflammation, inducing only viral infection- and replication-independent processes[38-40]. These models displayed mixed Th2, Th1, Th17 cell phenotypes, are not always responsive to high doses of systemic prednisone and do not consistently lead to asthma-like lung function deterioration.

In comparison to other models, our model reflects most key features of severe asthma exacerbation and provides complete and detailed kinetics on many cell subsets and immune mediators in the airways. In addition, we have mimicked natural infections by infection with low viral loads of X31, excluding possible altered responses upon high viral doses. Our model is also quite robust in the sense that data from four independent experiments was very similar and could be merged without losing information.

There are some limitations to the study. The changes in cell numbers over time after exposure to influenza may be associated with recruitment of cells as is supported by the coherent production of relevant chemokines. However, we cannot exclude the possibility that the increments of cells are due in part to a delayed apoptosis or reduced efflux of cells. Nevertheless, the early and marked increases of inflammatory mediators and cells in HDM-sensitized mice point to an exaggerated innate response upon influenza infection. Secondly, levels of the key innate mediator IL-33, a nuclear alarmin that can be induced and be released by various cell types such as epithelial cells, were profoundly increased in lung tissue and BALF. IL-33 in BALF is suggestive of its release, but its presence in lung tissue may also relate to mechanical and enzymatic treatment of lung tissue. These findings indicate that influenza infection results in marked production of IL-33, likely also by cells other than epithelial cells. Thirdly, lung function was assessed by whole body plethysmography as the Penh value, which is considered a surrogate marker of airways resistance. Nevertheless whole body plethysmography has been found to give reliable data in severe asthma models[41]. Also, as our focus was on inflammatory and immune processes this excluded the use of the flexivent system as those measurements are known to affect cell numbers. And finally, asthma is a heterogeneous disease and thus our model may be representative of a particular subtype of asthma. Clearly the choice of mouse strain may be a major factor affecting its representativeness of an asthma subtype. Currently we are performing transcriptome analyses

This article is protected by copyright. All rights reserved.

Accepted Article

on murine airway epithelial cells to see how well these analyses compare with analyses from primary bronchial epithelial cells from one or more asthma groups from the UBiopred study.

In conclusion, we have developed a murine model of virus-induced severe asthma exacerbations that recapitulates all major features of severe asthma exacerbations. An early innate mediator response in the airway lumen and an early eosinophil response apparently underlie the subsequent cellular and mediator responses. Furthermore, whereas anti-IL-5 in this model attenuates AHR and eosinophil numbers, we have shown a broad impact on other immune cells and viral load that provide novel intriguing insights into IL-5-driven pathways. We propose that this model can serve to discern the underlying mechanisms and aid the discovery of biological markers, development and testing the efficacy of novel interventions that can be translated to virus-induced severe asthma exacerbations.

Materials and Methods

Ethics Statement. All experiments described were approved by the Animal Research Ethics Board of the Academic Medical Center (protocol numbers DSK102810 and DSK49-AA) in adherence to the NIH Guide for the Care and Use of Laboratory Animals, performed according to institutional guidelines, EU and Netherlands legislation.

Mice, allergen, virus and treatments. Male 8 weeks old C57BL/6J mice purchased from Charles River Laboratories (France) were housed under specific pathogen-free conditions and maintained on a 12 hour light-dark cycle with access to food and water *ad libitum*. The sensitization schedule to elicit a severe and persistent eosinophilic allergic inflammation of the airways was based on the chronic HDM model first described by Johnson et al. and subsequently adapted.[16,157] In short, groups of C57BL/6J mice were randomly assigned to be treated for five days a week for five consecutive weeks with either the aeroallergen HDM (Greer Laboratories, Lenoir, NC, USA) or PBS through intranasal (i.n.) administration. Lyophilized HDM extract was resuspended in sterile PBS at a concentration of 5 mg (protein)/ml and 25 μg (5 μl) protein per dose per mouse was administered i.n. in a final volume of 20 μl (in PBS) in mice lightly anesthetized with isofluorane.

The H3N2 influenza A virus HK X31 stocks and viral titers were obtained by infecting Madin-Darby-Canine-Kidney (MDCK) as described before[42].

This article is protected by copyright. All rights reserved.

Accepted Article

The viral stock suspension was diluted in PBS and animals (lightly anesthetized with isofluorane) received i.n. 20 $TCID_{50}$ in 50 µl.

Fluticasone Propionate, a kind gift from Robert Shaw (GSK, Stevenage), was dissolved in sterile 0.05% Tween 20 in PBS and administered i.n. at a dose of 300ug/kg/ mouse in a volume of 20µl in mice lightly anesthetized with isofluorane. TRFK5, or the isotype control antibody, kind gifts from Robert Shaw (GSK, Stevenage), or Prednisone (Sigma-Aldrich) were diluted in sterile PBS and 5 mg/kg in 100 µl were administered separately via the intraperitoneal (i.p) route. Fluticasone Propionate (FP), Prednisone (Pred) and anti-IL5 (TRFK5) were given at different time points and with different routes of administration (i.n., i.p., i.p., respectively) because of their intrinsic pharmacodynamics and pharmacokinetic characteristics. These treatments are all therapeutic and not prophylactic. The different schedules for each treatment are based on extensive pilot studies on HDM-sensitized mice and X31-infected mice (Refractory Respiratory Inflammation DPU, Respiratory R&D, GSK, Stevenage, UK; data not published and kindly provided by Dr. Robert Shaw) and were expected to be efficacious, with evident beneficial anti-inflammatory effects, in the shortest period of administration and without eliciting serious side effects (i.e. body weight loss, misregulation of the immune function).

Airway responsiveness measurements. AHR responses were assessed at the indicated time points by methacholine-induced airflow obstruction in conscious mice placed in a whole-body plethysmograph (Buxco Electronics, Troy, NY) as described previously[43].

Specimens collection and primary cell isolation. For BALF collection mice were cannulated through the trachea and the lavage was performed by instilling and retrieving 1 mL of sterile saline into the right lung. BALF recovered exclusively from the right lung was centrifuged at 260 g for 10 min at 4°C and supernatants were stored at −80°C until further use, whereas the pellet was immediately resuspended in 0.2 mL of sterile PBS. Cell counts were then determined for each BALF sample by Trypan Blue staining, and differential cell counts were performed on cytospin preparations stained with modified Giemsa stain. For each BALF sample the cellular subset phenotypes were determined by staining with specific antibodies for cytofluorimetric analysis.

This article is protected by copyright. All rights reserved.

Accepted Article

To remove the intra-vascular pool of cells lungs were perfused with 5 mL of sterile saline via the pulmonary circulation, through catheterization of the right heart. Then the left lungs (not undergone BAL) and the mLNs were removed.

To prepare a lung homogenate, left lungs were minced using iridectomy scissors; lungs and mLNs were enzymatically digested for one hour at 37°C with Collagenase type III (200 U/ml, Worthington Biochemical Corp. Lakewood, NJ) and DNAse I (100 U/ml, grade II from bovine pancreas, Sigma) in RPMI 1640 medium. Pulmonary and lymph node cell suspensions were obtained by grinding the tissue through 70 µm nylon sieves and red blood cells were lysed using ammonium chloride buffer. Cell counts were then performed before staining for flow cytometry analysis.

The cell suspension was lysed using Greenberger buffer (75 mM NaCl, 7.5 mM Tris, 0.5 mM $MgCl_2$, 0.5 mM $CaCl_2$, 0.5% Triton X-100, 4 µg/ml 4-(2-aminoethyl)benzenesulfonyl fluoride, 50 µg/ml Na_2-EDTA, 10 ng/ml Pepstatin A, 10 ng/ml Leupeptin, pH 7.4) for 30 min on ice, followed by centrifugation at 680 g for 10 min. Supernatants were stored at −80°C until further use.**Flow cytometry analysis.** BALF, lungs and mLNs single cell suspensions were stained with CD3-BV510, CD4-BV650, CD8-BV711, CD19-BV786, CD11c-PE-Cy7, SiglecF-PE, CD11b-PE-CF594, CD80-APC, (BD Biosciences), CCR3-Alexa700 (R&D systems), MHCII-FITC (eBiosciences), CD86-APC Cy7 (Biolegend) in the presence of Fc blocker (CD16/CD32, Bioceros, Utrecht, NL). All appropriate isotype controls were used. Data was collected on a BD Biosciences Fortessa flow cytometer and analyzed using Flowjo software (Treestar and Stanford University, Palo Alto, CA).

Determination of viral outgrowth. Viral load was determined by real-time quantitative PCR in lung cell suspension as described previously[44]. The viral load present in a sample was calculated using a standard curve of particle-coated influenza virus included in every assay run. The following primers were used: 5'- GACAAGACCAATCCTGTCACYTCTG -3' (forward); 5'- AAGCGTCTACGCTGCAGTCC -3' (reverse), 5'- TTCACGCTCACCGTGCCCAGTGAGC -3'(50-FAM labeled probe).

Histopathological analysis. The left lungs from four additional animals per group, not undergone BAL and not used for FACS analysis, were harvested at the indicated time points, fixed overnight in 10% formalin and embedded in paraffin. Sections (4 µm) were stained

This article is protected by copyright. All rights reserved.

Accepted Article

with hematoxylin and eosin (H&E) and Periodic Acid-Schiff (PAS). Multiple images of the primary airway were taken with OpenLab software (version 3.0.3; Improvision) via a camera and microscope (Leica Microsystems).

Cytokine and chemokines analysis. Levels of cytokines and chemokines in BALF and lung homogenates were measured using a Luminex 100 Total System based on xMAP multiplexing technology with Bio-Plex Pro Mouse 8-Plex Panel and Bio-Plex Pro Mouse 23-Plex Panel assays kits (Bio-Rad Laboratories Ltd. UK) or by ELISA (HK2010 mouse MPO kit, Hycult biotech) according to manufacturers' specifications.

Data analysis. Data are expressed as mean ± SEM. Results were interpreted using ANOVA and Bonferroni's difference post hoc test (Prism 5, GraphPad). Differences were considered statistically significant when $p<0.05$. Experiments were conducted with four to six mice per group per time point and data are representative at least four independent replicates unless differently indicated (e.g. Fig. 2 and Fig. 4, five and two replicates, respectively). The numbers of mice used are indicated in the figure legends.

References

1. Jackson DJ, Sykes A, Mallia P, Johnston SL. Asthma exacerbations: origin, effect, and prevention. J Allergy Clin Immunol 2011;128:1165-74.
2. <International ERS ATS Guidelines on Definition, Evaluation and Treatment of Severe Asthma 2013.pdf>.
3. Masoli M, Fabian D, Holt S, Beasley R, Global Initiative for Asthma P. The global burden of asthma: executive summary of the GINA Dissemination Committee report. Allergy 2004;59:469-78.
4. Dougherty RH, Fahy JV. Acute exacerbations of asthma: epidemiology, biology and the exacerbation-prone phenotype. Clin Exp Allergy 2009;39:193-202.
5. Johnston SL, Pattemore PK, Sanderson G, et al. Community study of role of viral infections in exacerbations of asthma in 9-11 year old children. BMJ 1995;310:1225-9.
6. Mahut B, Refabert L, Marchac V, et al. Influenza-like illness responsible for severe exacerbations in asthmatic children during H1N1 pandemic: a survey before vaccination. J Asthma 2011;48:224-7.
7. Sandrock CE, Norris A. Infection in severe asthma exacerbations and critical asthma syndrome. Clin Rev Allergy Immunol 2015;48:104-13.
8. Matsuse H, Tsuchida T, Fukahori S, et al. Differential airway inflammatory responses in asthma exacerbations induced by respiratory syncytial virus and influenza virus a. Int Arch Allergy Immunol 2013;161:378-82.
9. Fleming DM, Pannell RS, Elliot AJ, Cross KW. Respiratory illness associated with influenza and respiratory syncytial virus infection. Archives of Disease in Childhood 2005;90:741-6.

This article is protected by copyright. All rights reserved.

Accepted Article

10. Zhu J, Message SD, Qiu Y, et al. Airway inflammation and illness severity in response to experimental rhinovirus infection in asthma. Chest 2014;145:1219-29.
11. Singh AM, Busse WW. Asthma exacerbations. 2: aetiology. Thorax 2006;61:809-16.
12. Bel EH, Wenzel SE, Thompson PJ, et al. Oral glucocorticoid-sparing effect of mepolizumab in eosinophilic asthma. N Engl J Med 2014;371:1189-97.
13. Chung KF, Wenzel SE, Brozek JL, et al. International ERS/ATS guidelines on definition, evaluation and treatment of severe asthma. Eur Respir J 2014;43:343-73.
14. Pavord ID, Korn S, Howarth P, et al. Mepolizumab for severe eosinophilic asthma (DREAM): a multicentre, double-blind, placebo-controlled trial. Lancet 2012;380:651-9.
15. Johnson JR, Wiley RE, Fattouh R, et al. Continuous exposure to house dust mite elicits chronic airway inflammation and structural remodeling. Am J Respir Crit Care Med 2004;169:378-85.
16. Ulrich K, Hincks JS, Walsh R, et al. Anti-inflammatory modulation of chronic airway inflammation in the murine house dust mite model. Pulm Pharmacol Ther 2008;21:637-47.
17. FitzGerald JM, Gibson PG. Asthma exacerbations . 4: Prevention. Thorax 2006;61:992-9.
18. Haldar P, Brightling CE, Hargadon B, et al. Mepolizumab and exacerbations of refractory eosinophilic asthma. N Engl J Med 2009;360:973-84.
19. Pavord ID, Haldar P, Bradding P, Wardlaw AJ. Mepolizumab in refractory eosinophilic asthma. Thorax 2010;65:370.
20. Monticelli LA, Sonnenberg GF, Abt MC, et al. Innate lymphoid cells promote lung-tissue homeostasis after infection with influenza virus. Nat Immunol 2011;12:1045-54.
21. Enomoto Y, Orihara K, Takamasu T, et al. Tissue remodeling induced by hypersecreted epidermal growth factor and amphiregulin in the airway after an acute asthma attack. J Allergy Clin Immunol 2009;124:913-20 e1-7.
22. Pulendran B, Artis D. New paradigms in type 2 immunity. Science 2012;337:431-5.
23. Aldington S, Beasley R. Asthma exacerbations. 5: assessment and management of severe asthma in adults in hospital. Thorax 2007;62:447-58.
24. Jackson DJ, Makrinioti H, Rana BMJ, et al. IL-33–Dependent Type 2 Inflammation during Rhinovirus-induced Asthma Exacerbations In Vivo. American Journal of Respiratory and Critical Care Medicine 2014;190:1373-82.
25. Johnston SL. Innate immunity in the pathogenesis of virus-induced asthma exacerbations. Proc Am Thorac Soc 2007;4:267-70.
26. Carretero R, Sektioglu IM, Garbi N, Salgado OC, Beckhove P, Hammerling GJ. Eosinophils orchestrate cancer rejection by normalizing tumor vessels and enhancing infiltration of CD8(+) T cells. Nat Immunol 2015;16:609-17.
27. Schwantes EA, Manthei DM, Denlinger LC, et al. Interferon gene expression in sputum cells correlates with the Asthma Index Score during virus-induced exacerbations. Clin Exp Allergy 2014;44:813-21.
28. Dyer KD, Czapiga M, Foster B, et al. Eosinophils from lineage-ablated Delta dblGATA bone marrow progenitors: the dblGATA enhancer in the promoter of GATA-1 is not essential for differentiation ex vivo. J Immunol 2007;179:1693-9.
29. Hogan SP, Rosenberg HF, Moqbel R, et al. Eosinophils: biological properties and role in health and disease. Clin Exp Allergy 2008;38:709-50.
30. Percopo CM, Dyer KD, Karpe KA, Domachowske JB, Rosenberg HF. Eosinophils and respiratory virus infection: a dual-standard curve qRT-PCR-based method for

This article is protected by copyright. All rights reserved.

Accepted Article

determining virus recovery from mouse lung tissue. Methods Mol Biol 2014;1178:257-66.
31. Fukumoto J, Harada C, Kawaguchi T, et al. Amphiregulin attenuates bleomycin-induced pneumopathy in mice. Am J Physiol Lung Cell Mol Physiol 2010;298:L131-8.
32. Bartlett NW, Walton RP, Edwards MR, et al. Mouse models of rhinovirus-induced disease and exacerbation of allergic airway inflammation. Nat Med 2008;14:199-204.
33. Kumar RK, Herbert C, Foster PS. The "classical" ovalbumin challenge model of asthma in mice. Curr Drug Targets 2008;9:485-94.
34. Nials AT, Uddin S. Mouse models of allergic asthma: acute and chronic allergen challenge. Dis Model Mech 2008;1:213-20.
35. Jungsuwadee P, Benkovszky M, Dekan G, Stingl G, Epstein MM. Repeated aerosol allergen exposure suppresses inflammation in B-cell-deficient mice with established allergic asthma. Int Arch Allergy Immunol 2004;133:40-8.
36. Nguyen TH, Maltby S, Simpson JL, et al. TNF-alpha and Macrophages Are Critical for Respiratory Syncytial Virus-Induced Exacerbations in a Mouse Model of Allergic Airways Disease. J Immunol 2016;196:3547-58.
37. Hasegawa S, Wakiguchi H, Okada S, et al. Cytokine profile of bronchoalveolar lavage fluid from a mouse model of bronchial asthma during seasonal H1N1 infection. Cytokine 2014;69:206-10.
38. Clarke DL, Davis NH, Majithiya JB, et al. Development of a mouse model mimicking key aspects of a viral asthma exacerbation. Clin Sci (Lond) 2014;126:567-80.
39. De Alba J, Otal R, Calama E, et al. Double-stranded RNA evokes exacerbation in a mouse model of corticosteroid refractory asthma. Clin Sci (Lond) 2015;129:973-87.
40. Mahmutovic Persson I, Akbarshahi H, Menzel M, Brandelius A, Uller L. Increased expression of upstream TH2-cytokines in a mouse model of viral-induced asthma exacerbation. J Transl Med 2016;14:52.
41. Verheijden KA, Henricks PA, Redegeld FA, Garssen J, Folkerts G. Measurement of airway function using invasive and non-invasive methods in mild and severe models for allergic airway inflammation in mice. Front Pharmacol 2014;5:190.
42. Bodewes R, Kreijtz JH, Baas C, et al. Vaccination against human influenza A/H3N2 virus prevents the induction of heterosubtypic immunity against lethal infection with avian influenza A/H5N1 virus. PLoS One 2009;4:e5538.
43. Hansen G, Berry G, DeKruyff RH, Umetsu DT. Allergen-specific Th1 cells fail to counterbalance Th2 cell-induced airway hyperreactivity but cause severe airway inflammation. J Clin Invest 1999;103:175-83.
44. van der Sluijs KF, van Elden L, Nijhuis M, et al. Toll-like receptor 4 is not involved in host defense against respiratory tract infection with Sendai virus. Immunol Lett 2003;89:201-6.

Acknowledgements: The authors gratefully acknowledge Dr. Robert Shaw (Refractory Respiratory Inflammation DPU, Respiratory R&D, GSK, Stevenage, UK) for support in providing reagents and defining the experimental set-up, for insightful discussions and for constructive comments on the manuscript. Authors are also grateful to Dr. M.A. van de Pol (Academic Medical Centre, Amsterdam) for the technical support in the multiplex assays and M. Bombaci (INGM, Milan) for assistance with data analysis.

This article is protected by copyright. All rights reserved.

Accepted Article

Funding: The study is supported by Chiesi Farmaceutici S.p.A. and the U-BIOPRED consortium that receives funding from the European Community and from the European Federation of Pharmaceutical Industries and Associations as an IMI JU funded project.

Author contributions: L.R. devised and conducted the study, provided flow cytometric analyses, analyzed the data and prepared the manuscript, A.D. provided animals treatment and primary cells isolation, Y.S.S.P, S.M.B., B.S.D. and T.D. performed *in vitro* analysis and provided associated data, A.L. contributed to the AHR measurments, L.B. provided reagents for FACS analysis, G.V. and F.F contributed to the experimental set-up definition, I.M.A., N.L.R., P.J.S. prepared the manuscript, R.L devised the study, contributed to the experimental set-up definition and prepared the manuscript. All authors approved the final version of the manuscript. **Competing interests:** The authors declare that they have no competing interests.

Conflicts of interest: Navin L Rao is employed by Janssen Research and Development LLC, Louis Boon by Bioceros, Gino Villetti and Fabrizio Facchinetti by Chiesi Farmaceutici S.p.A. All other authors have any finantila discousures to declare.

This article is protected by copyright. All rights reserved.

Accepted Article

Accepted Article

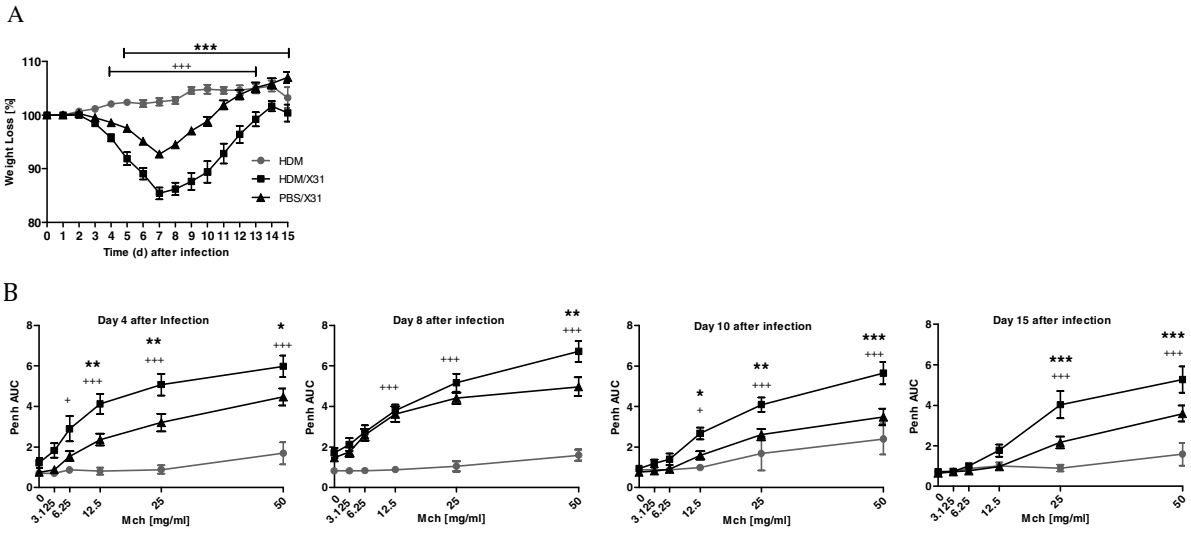
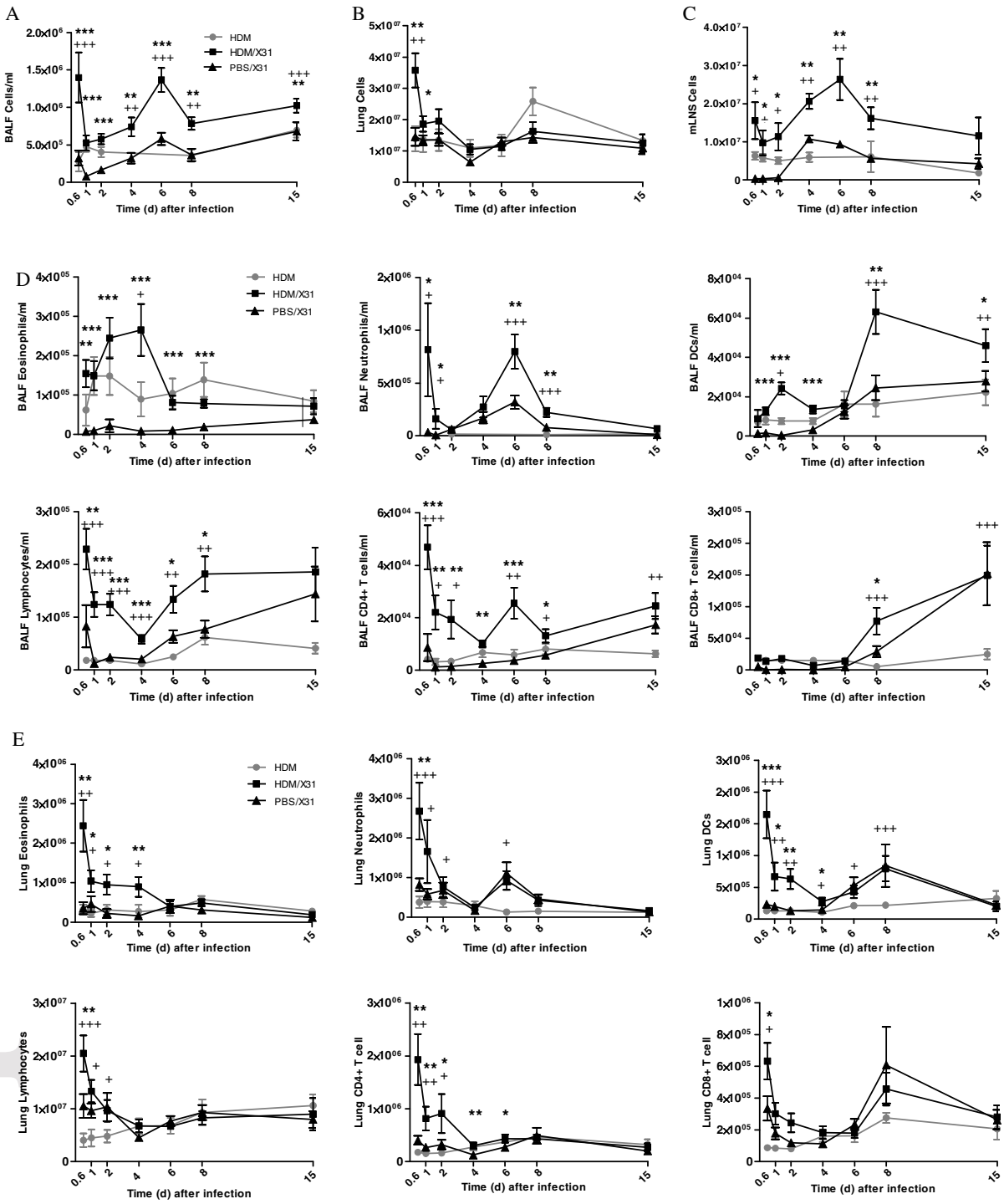


Figure 1. Influenza aggravates loss of bodyweight and airway hyper-responsiveness (AHR) in a model of chronic allergic airway inflammation. C57BL/6J mice were exposed for 5 days a week for 5 consecutive weeks to house dust mite extract (HDM) or treated with PBS (PBS) intranasally (i.n.) and subsequently infected (i.n.) with influenza virus X31 (HDM/X31 or PBS/X31, respectively) on day 29 of the sensitization schedule. (A) Bodyweight loss during the experiment. (B) AHR to increasing doses of methacholine (Mch) was assessed on days 4, 8, 10 and 15 post X31 infection reflected by Penh area under the curve (AUC). Data are representative of 4 independent experiments with 4 mice per time point and are expressed as means ± SEM (2 way ANOVA followed by Bonferroni's post-test to compare all groups); *p<0.05, **p<0.01, ***p<0.001 for the comparison between HDM/X31 and PBS/X31; +p<0.05, ++p<0.01, +++p<0.001 for the comparison between HDM/X31 and HDM/PBS.

This article is protected by copyright. All rights reserved.

Accepted Article



This article is protected by copyright. All rights reserved.

F

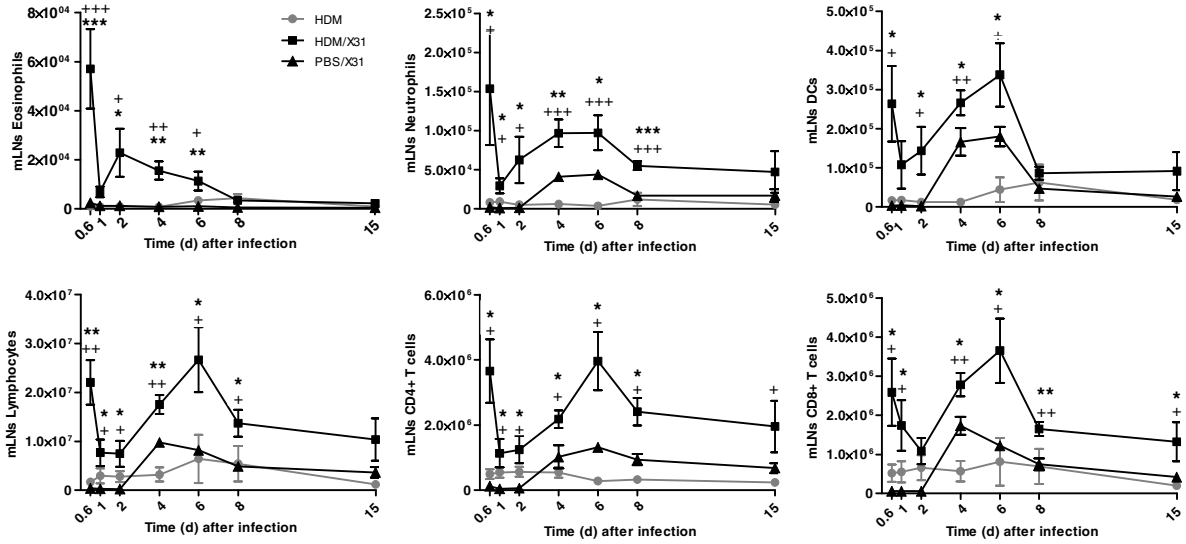
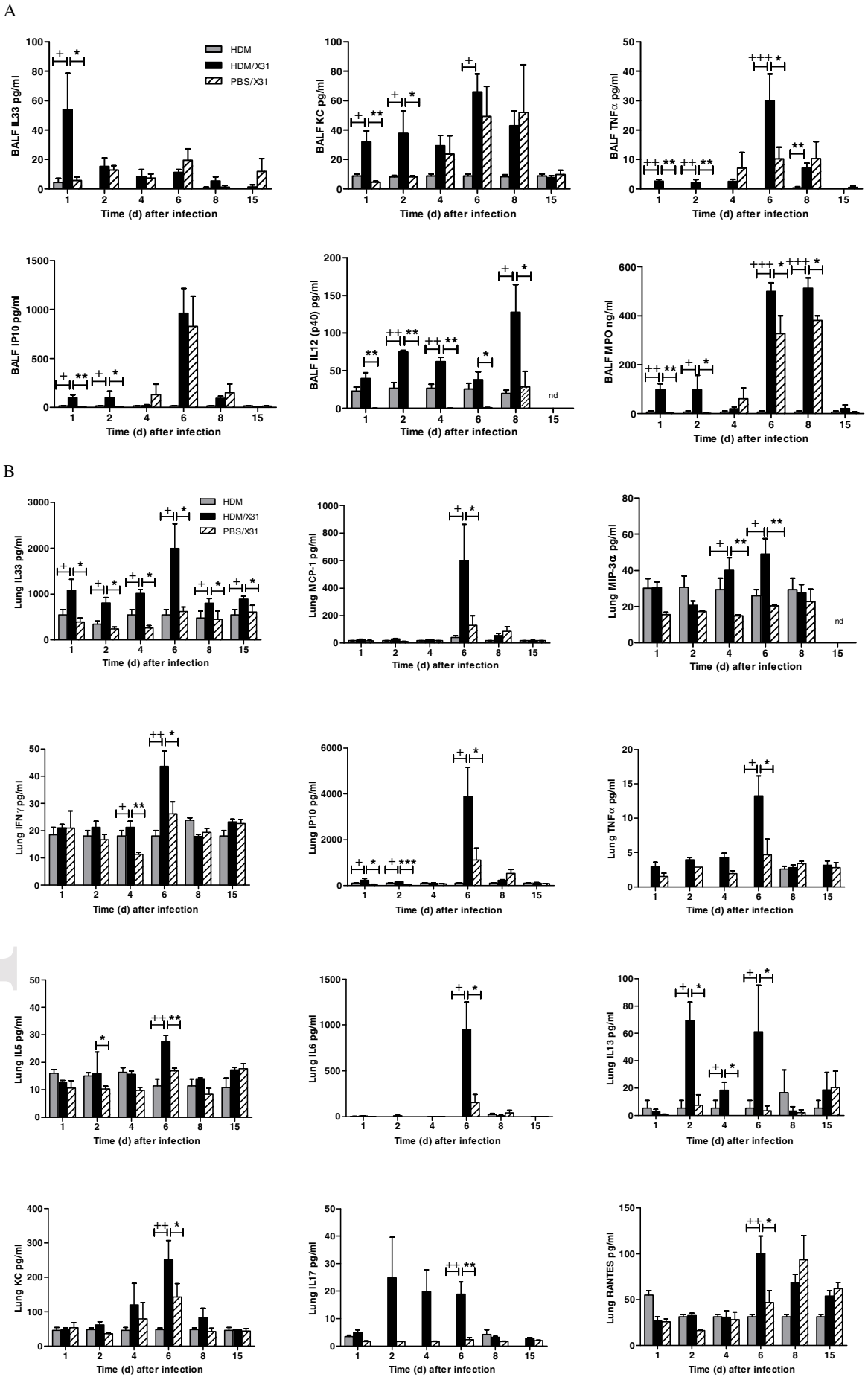


Figure 2. Influenza enhances inflammatory cell influx into the airway lumen, lung parenchyma and draining lymph nodes from HDM-sensitized mice.
C57BL/6J mice sensitized (i.n.) to either HDM, or PBS control, were subsequently infected with X31 (HDM/X31 or PBS/X31, respectively) on day 29 of the sensitization schedule. Total cell counts in the airway lumen (BALF;(A),) lung parenchyma (lung; (B)) and mediastinal draining lymph nodes (mLNs; (C)) were assessed at indicated time points after X31 infection. BALF (D), lung (E) and mLNs (F) samples were analyzed by flow cytometry to determine the kinetics of eosinophils, neutrophils, DCs, total lymphocytes and T cells over time after X31 infection. Data are representative of 5 independent experiments with 4 to 6 mice per group and are presented as means ± SEM (2 way ANOVA followed by Bonferroni's post-test to compare all groups); *p<0.05, **p<0.01, ***p<0.001 for the comparison between HDM/X31 and PBS/X31; +p<0.05, ++p<0.01, +++p<0.001 for the comparison between HDM/X31 and HDM controls.

Accepted Article

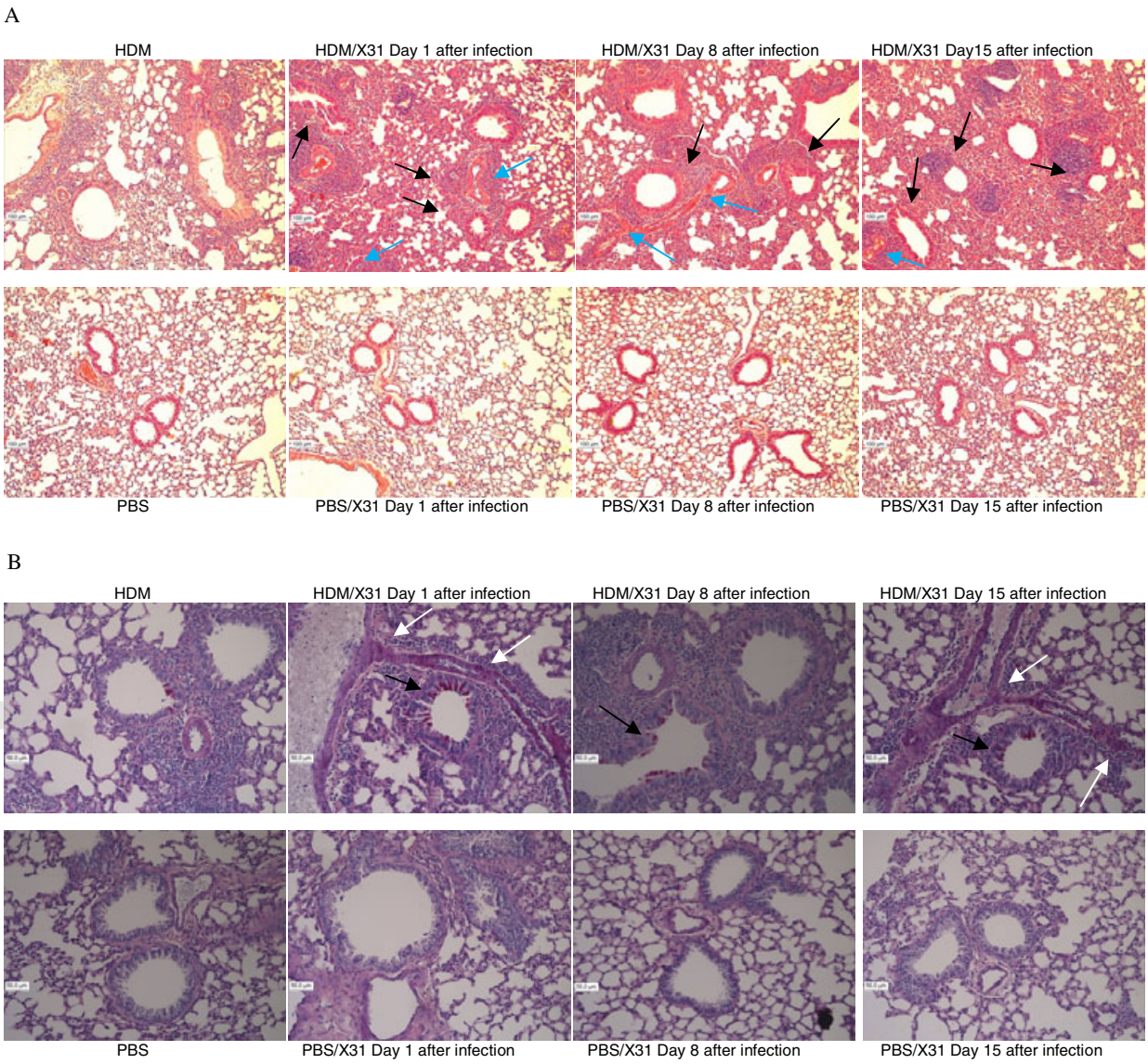
This article is protected by copyright. All rights reserved.

Accepted Article



This article is protected by copyright. All rights reserved.

Figure 3. Influenza enhances inflammatory mediators in BALF and lung parenchyma from HDM-sensitized mice. C57BL/6J mice sensitized (i.n.) to HDM for 5 days a week for 5 consecutive weeks or treated with PBS were infected with X31 (HDM/X31 or PBS/X31, respectively) on day 29 of the sensitization schedule. IL-33, KC, TNF-α, IL-12p40, IP10/CXCL10 and MPO were quantified in cell-free BALF over time (A). Similarly, IL-33, MCP-1/CCL2, MIP-3α/CCL20, IL-5, IL-6, IL-13, IFN-γ, IP10, TNF-α, KC, IL-17 and RANTES were determined in lung parenchyma (B). Chemokines and cytokines were determined by luminex and MPO by ELISA. Data are representative of 3 independent experiments of 4 or 6 mice per group and is presented as means ± SEM; *p<0.05, **p<0.01, ***p<0.001 for the comparison between HDM/X31 and PBS/X31; +p<0.05, ++p<0.01, +++p<0.001 for the comparison between HDM/X31 and HDM controls. n.d.: not detectable.



This article is protected by copyright. All rights reserved.

Accepted Article

C

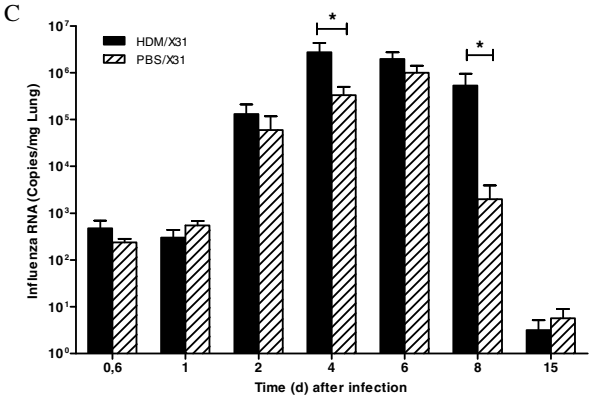


Figure 4. Influenza aggravates lung pathology and yields more viral replicates in HDM-sensitized mice. C57BL/6J mice sensitized (i.n.) with HDM 5 days a week for 5 consecutive weeks or treated with PBS were infected with X31 (HDM/X31 or PBS/X31, respectively) on day 29 of the sensitization schedule. H&E (A) and PAS staining (B) of perfused lungs from the four groups. X31 infection in HDM mice led to peribronchial (black arrow) and perivascular (blue arrow) inflammation (A). Mucous production (magenta) by epithelial goblet cells (black arrow) and vascular occlusive lesions (white arrow) were also enhanced (B). Scale bars, 50μm. Images shown are representative of three mice. (C) Longitudinal quantification of X31 viral load in lung homogenates by quantitative RT-PCR. Data are means ± SEM. and representative of four experiments with groups of four mice; *P <0.05, **P < 0.01 and ***P < 0.001 for HDM/X31 mice compared with PBS/X31 controls.

This article is protected by copyright. All rights reserved.

Accepted Article

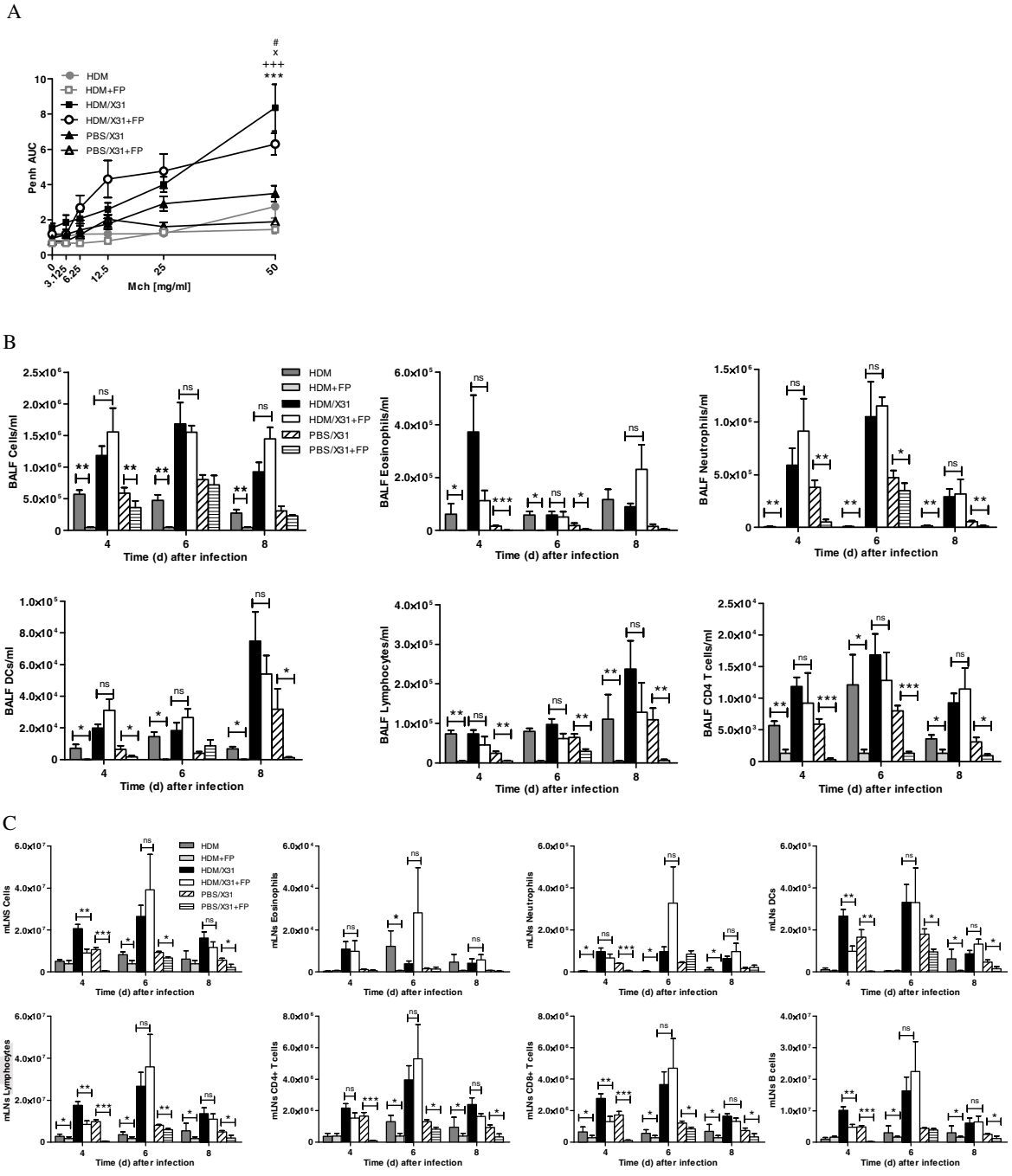


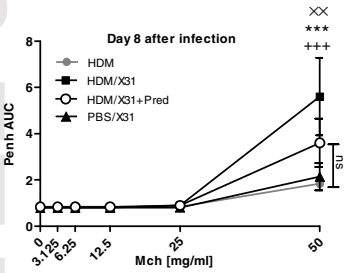
Figure 5. Fluticasone Propionate (FP) fails to attenuate AHR and immune and inflammatory cells recruitment in HDM/X31 mice. Mice sensitized (i.n.) with HDM for 5 days a week for 5 consecutive weeks, or administrated with PBS, were treated (i.n.) with FP from day 22 of the sensitization schedule and then infected with X31 (HDM/X31 or PBS/X31, respectively) on day 29. (A) FP did not attenuate AHR in HDM/X31 mice, whereas AHR in HDM-sensitized and PBS/X31 animals was reduced at day 8 post-infection. Data represent means ± SEM (2 way ANOVA followed by Bonferroni's post-test to compare all groups) for groups of four mice; ***p<0.001 for the comparison between HDM/X31 and

This article is protected by copyright. All rights reserved.

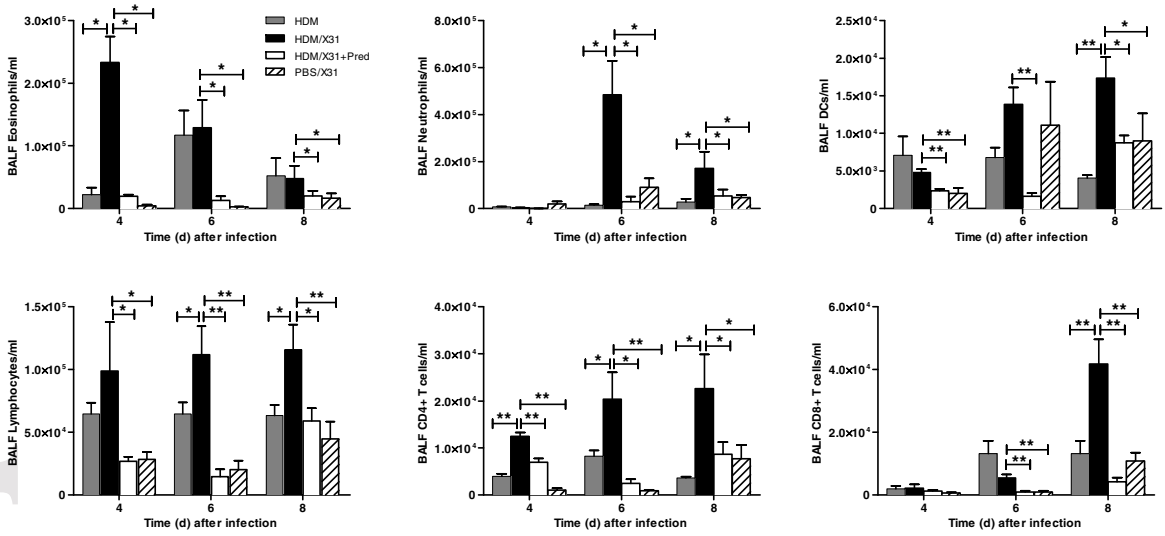
PBS/X31; +++p<0.001 for the comparison between HDM/X31 and HDM; $^{\times}$p<0.05 for the comparison between HDM and HDM+FP; $^{\#}$p<0,05 for the comparison between PBS/X31and PBS/X31+FP.

Cells from BALF (B) and mLNs (C) were analyzed by flow cytometry. Recruitment of granulocytes and lymphocytes was not attenuated by FP in HDM/X31 mice, while it was in HDM-sensitized or PBS/X31mice. All data are representative of 4 replicates of independent experiments for groups of 4 mice. Data represent means ± SEM (*t*-test); *p<0.05, **p<0.01, ***p<0.001 for the comparison between the indicated groups.

A



B



This article is protected by copyright. All rights reserved.

C

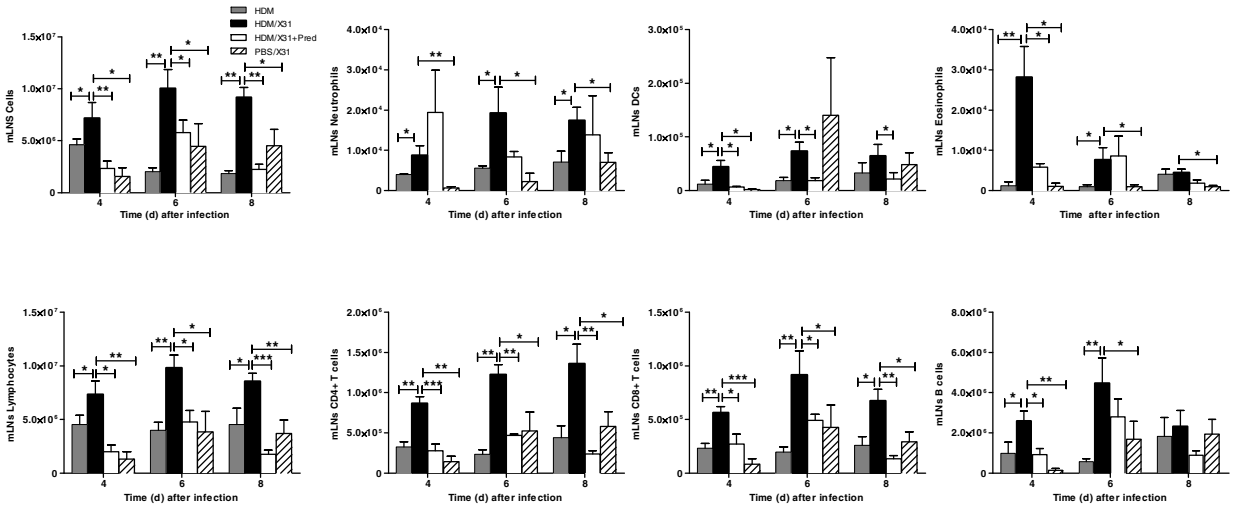
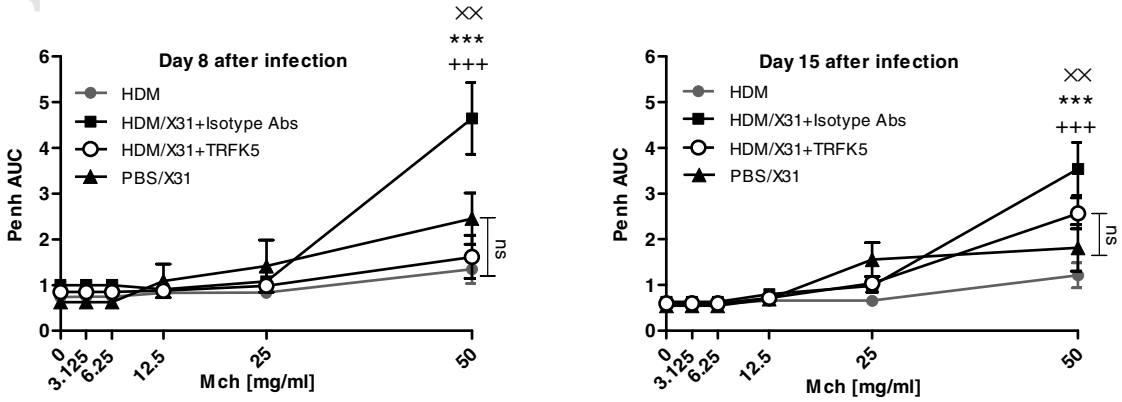


Figure 6. Systemic Prednisone (Pred) controls AHR and immune and inflammatory cells in HDM/X31 mice. Mice sensitized (i.n.) with HDM for 5 days a week for 5 consecutive weeks, or administrated with PBS, were treated with Pred (as from day 25 of the sensitization schedule). (A) Pred reduced AHR of HDM/X31 mice at day 8 post-infection. Data represent means ± SEM (2 way ANOVA followed by Bonferroni's post-test to compare all groups) for groups of four mice; ***p<0.001 for the comparison between HDM/X31 and PBS/X31; +++p<0.001 for the comparison between HDM/X31and HDM; $^{\times\times}$p<0.01 for the comparison between HDM/X31 and HDM/X31+Pred. Cells from BALF (B) and mLNs (C) were analyzed by flow cytometry. Recruitment of granulocytes and lymphocytes was attenuated by Pred in HDM/X31 mice between days 4 to 8 post-infection. Data represent means ± SEM of groups of four mice (*t*-test); *p<0.05, **p<0.01, ***p<0.001 for the comparison between the indicated groups.

A



This article is protected by copyright. All rights reserved.

B

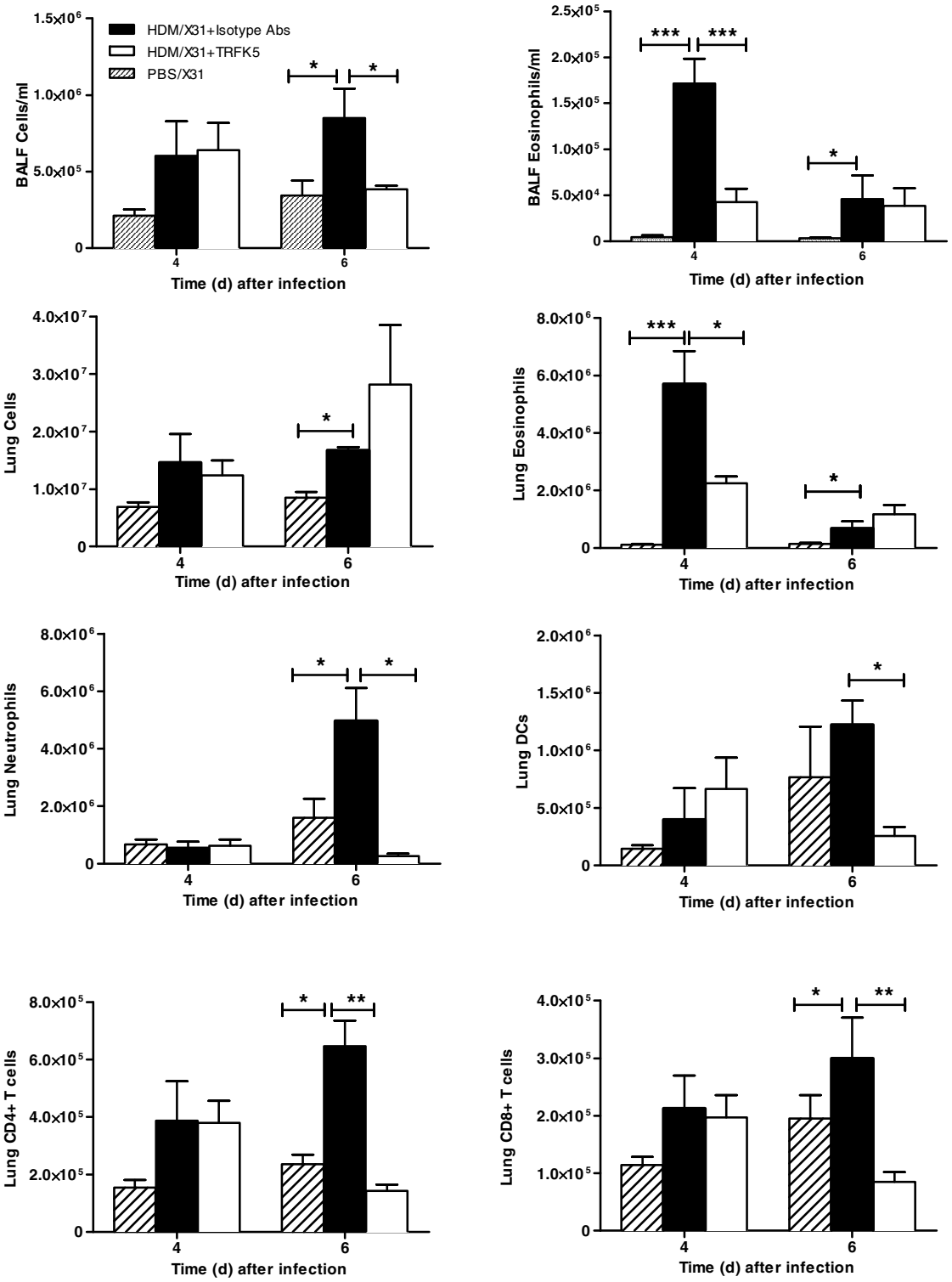
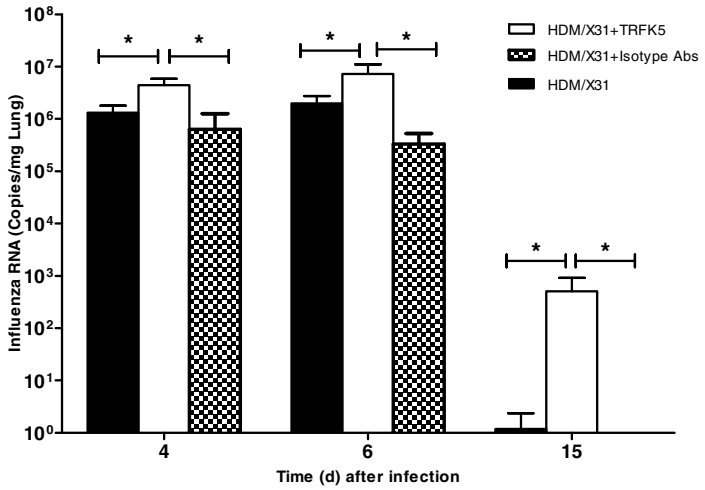


Figure 7. The murine αIL5-mAb TFRK5 attenuates AHR and modulates immune and inflammatory cells in HDM/X31 mice. Mice sensitized (i.n.) with HDM for 5 days a week for 5 consecutive weeks, or administrated with PBS, were treated were treated systemically

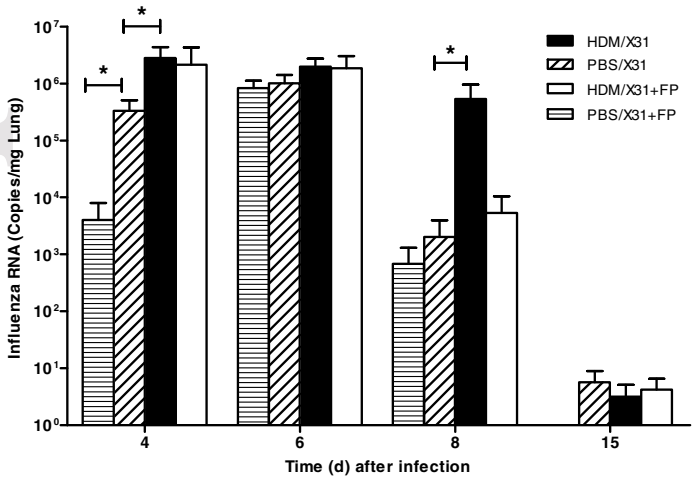
This article is protected by copyright. All rights reserved.

with TRFK5 (on day 26 and 32). (A) TRFK5 reduced AHR of HDM/X31 mice at days 8 and 15 post-infection. Data presented as means ± SEM (2 way ANOVA followed by Bonferroni's post-test to compare all groups) for groups of four mice; ***p<0.001 for the comparison between HDM/X31 and PBS/X31; +++p<0.001 for the comparison between HDM/X31 and HDM; $^{\times\times}$p<0.01 for the comparison between HDM/X31+isotype and HDM/X31+TRFK5. (B) Cells were analyzed by flow cytometry in (B) BALF and lung. BALF eosinophils were attenuated by TRFK5 in HDM/X31 mice at day 4 but not at day 6 post-infection, whereas BALF total cell number was reduced at day 6 and neutrophils were enhanced. Lung eosinophils were reduced by TRFK5 at day 4, and DCs, neutrophils, CD4+ and CD8+ lymphocytes were reduced at day 6 as compared to isotype controls. Data are presented as means ± SEM of groups of four mice (*t*-test); *p<0,05, **p<0,01, ***p<0,001 for the comparison between the indicated groups.

A



B



C

This article is protected by copyright. All rights reserved.

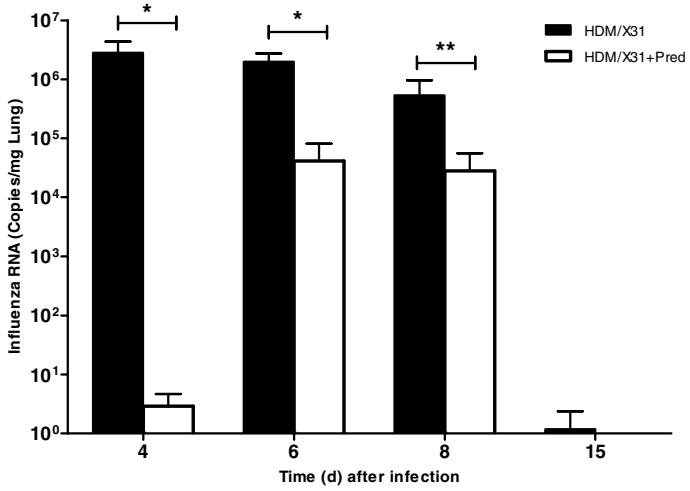


Figure 8. Effect of corticosteroids and anti-IL5 on influenza load in HDM Flu mice and controls. Viral load in lung homogenates were determined by quantitative RT-PCR. (A) Mice treated with anti-IL5 antibody (TRFK5) or (B) inhaled Fluticasone Propionate (FP) or (C) systemic prednisone (Pred) respectively. Data are presented as means ± SEM of groups of four mice (*t*-test); *p<0,05, for the comparison between the indicated groups at the indicated time points.

Accepted Article

This article is protected by copyright. All rights reserved.

Accepted Article

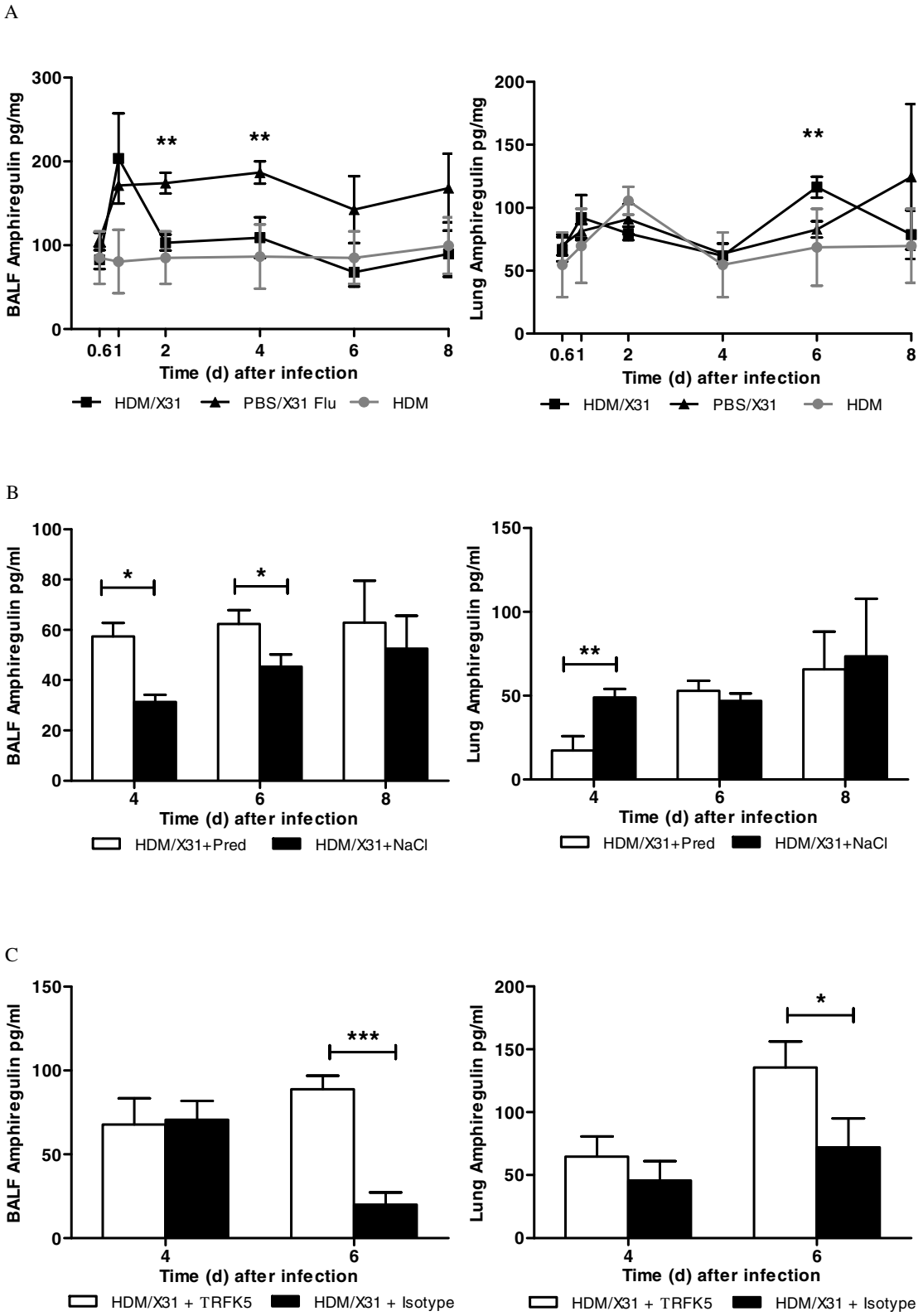


Figure 9. Influenza impairs luminal amphiregulin in HDM/X31 mice, which is restored by Pred and TRFK5 treatment. C57BL/6J mice sensitized (i.n.) with HDM for 5 days a week for 5 consecutive weeks or treated with PBS were infected with X31 (HDM/X31 or PBS/X31, respectively) on day 29 of the sensitization schedule (A). HDM/X31 or PBS/X31 mice were treated systemically with Pred (B) (from day 25 of the sensitization schedule) or with TRFK5 (C) (on day 26 and 32). Amphiregulin was quantified by ELISA in cell-free

This article is protected by copyright. All rights reserved.

BALF and in lung parenchyma, following enzymatic digestion. All data are representative of 3 independent experiments of 4 mice per group. Data are presented as means ± SEM; *p<0.05, **p<0.01, ***p<0.001 for the comparison between HDM Flu and PBS Flu, or HDM Flu and HDM/X31+ SCS, or HDM/X31 and HDM/X31+ TRFK5; +p<0.05, ++p<0.01, +++p<0.001 for the comparison between HDM/X31 and HDM.

Accepted Article

This article is protected by copyright. All rights reserved.